Extremely long-lived charge donor states formed by visible irradiation of quantum dots

Micaela K. Homer,[a] Helen C. Larson,[a] Grant J. Dixon,[a] Emily L. Miura-Stempel,[a] Neal R. Armstrong,[b] Brandi M. Cossairt*[a]

[a]Department of Chemistry, University of Washington, Seattle, WA 98195, United States

[b]Department of Chemistry and Biochemistry, University of Arizona, Tucson, AR 85721, United States

E-mail: *cossairt@uw.edu

Abstract

Using cyclic voltammetry under illumination, we recently demonstrated that CdS quantum dots (QDs) form charge donor states that live for at least several minutes after illumination ends, ~12 orders of magnitude longer than expected for free carriers. This timescale suggests that the conventionally accepted mechanism of charge transfer, wherein charges directly transfer to an acceptor following exciton dissociation, cannot be complete. Because of these long timescales, this unconventional pathway is not readily observed using time-resolved spectroscopy to probe charge transfer dynamics. Here, we investigated the chemical nature of these charge donor states using cyclic voltammetry under illumination coupled with NMR spectroscopy, X-ray diffraction, X-ray photoelectron spectroscopy, and optical spectroscopy. Our data reveal that charges are stored locally rather than as free carriers, and the number of charges stored is dependent on the QD surface ligation and stoichiometry. Altogether, our results confirm that electrons are stored at ligated surface Cd, these sites are competent charge donors, and this storage is charge balanced by X-type ligand desorption. We found that charge storage occurs in every QD system studied, including CdS, CdSe, and InP capped with carboxylate and phosphonate ligands.

Introduction

Interfacial charge transfer from quantum dots (QDs) has garnered attention in the last several decades because it is a key process in many applications such as photovoltaics,[1] photodetectors,[2] light-emitting technologies,[3] and photoredox catalysis.[4] Chemists often idealize photoinduced charge transfer through a two-state, Marcus-type event in which an excited electron (or hole) moves from the conduction band (valence band) edge to an external acceptor. The expansion of this model recently culminated in a review by Wu *et al.*, where the many complications of this simple picture are presented.[5] However, we note that much of the research in this field still focuses on using optical spectroscopy to track the charge carriers' migration from the QD on relatively short timescales (ps-μs). Insights from these studies are unable to capture longer timescale processes, which become relevant in any practical use of these materials in the applications listed above.

Previously, we reported a method to measure photoinduced charge transfer from CdS QDs to redox-active molecules using cyclic voltammetry (CV) under illumination.[6] This measurement allowed us to quantify effective, bimolecular charge transfer on the same timescale as chemical reactions by observing distortion of the CV of the redox-active molecule during illumination. The measurement is performed as follows: an electrolyte solution containing QDs and a one-electron molecular redox probe (e.g., ferrocene, Fc) is loaded into a three-electrode cell equipped with an LED that allows for simultaneous illumination and electrochemical measurement. CVs are taken before, during, and after illumination, and the shape of the CV distorts from the reversible shape in a manner consistent with adding a chemical reaction (charge transfer) to the reversible faradaic process (**Figure 1a**). Ferrocene is faradaically oxidized to form ferrocenium (Fc^+), which can be reduced by a photogenerated charge donor, QD*. The extent of the CV distortion corresponds to the observed rate of charge transfer from QD to molecular redox probe.

An unexpected finding from this measurement was the gradual distortion of CV during illumination, occurring over timescales much longer than exciton formation, *ca.* 30 minutes. Moreover, this distortion persisted for *ca.* 30 minutes after illumination stopped (**Figure 1b,c**). These slow changes to CV were consistent with the amount of charge donating species (QD*) in solution increasing during illumination for much longer than excitation and the charge donating species persisted for much longer than excitonic decay. This was true for both electron- and hole-transfer. These observations challenge conventionally held beliefs that charge transfer must proceed directly after excitation and be faster than carrier trapping. The following work aims to understand the chemical processes undergone by the QD during illumination that allow for charge transfer to occur long after illumination stops.

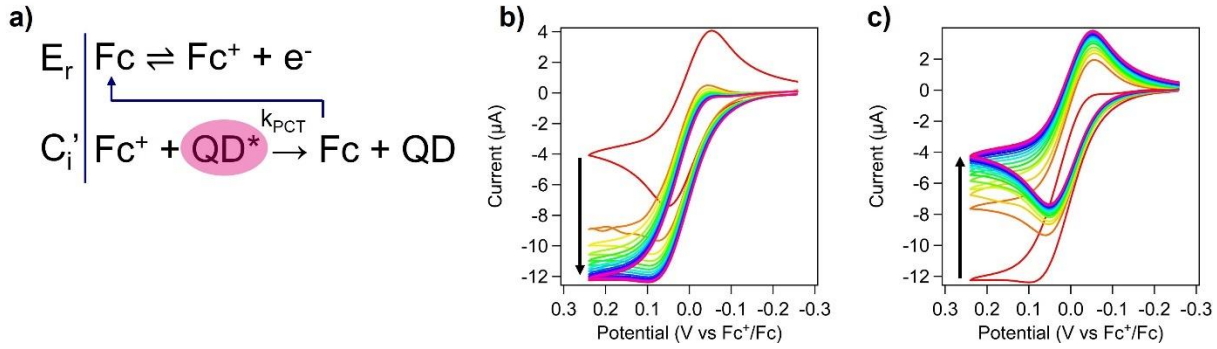

Figure 1. (a) The E_rC_i' mechanism we used to explain changes to the voltammogram upon illumination, where QD* refers to the charge donor species investigated in this work. **(b)** CVs of ferrocene distort to an S-shaped CV after illumination is turned on over *ca.* 30 minutes. There were 130 seconds between the start of one scan and the start of the next. **(c)** Slow recovery from S-shaped CV to reversible shape over *ca.* 30 minutes after illumination ends. CV data shown are original to this work.

Others have observed similar long-lived reactivity after illumination in other materials, which has been termed "dark photocatalysis" or "photocatalytic memory."[7] The most common system consists of a semiconductor that acts as the light sensitizer and an energy-storing substance that can store photo-generated charge carriers during illumination and slowly release those carriers in

the dark.[7,8] There are many examples of nanocrystals acting as semiconductors in dark photocatalytic systems.[9–18] However, systems where the light absorber is the same as the energy storage material are rarely reported, and in these, the identity of the charge-storing species was not explored.[19,20] Our observations fall into the category of dark photocatalysis, but we have uniquely observed this behavior intrinsically on QDs.

Photoinduced changes to QDs on long timescales have been well-investigated in relation to their photoluminescence behavior. Photobrightening[21–27] is the process in which the photoluminescence quantum yield increases over minutes to hours of QD illumination. There is more than one mechanism behind this phenomenon, though the general description of photobrightening is that irradiation smooths the QD core's surface and removes or passivates surface defects. This decrease in surface trapping may be thermal (photoannealing), or the charge carriers generated during illumination may remove surface states through trap filling or other surface redox reactions.[28] Related processes include photodarkening[29] and photoluminescence blinking,[30,31] where similar photoinduced surface redox activity causes PL changes over timescales longer than exciton generation and decay. It seems reasonable that the photoinduced surface redox processes that affect PL may be chemically related to the processes that slowly generate long-lived charge donors. Altogether, we hypothesized the redox-active surface of the QDs may act as the intermediate between exciton dissociation and charge transfer.

Considering our prior observations of these long-lived charge donor states, we sought to understand the ubiquity of this effect and gain a chemical understanding of this new mechanism for photoinduced charge storage and transfer. We considered the three mechanisms presented in **Scheme 1** as well as several more rejected mechanisms presented in **SI Scheme 1**. We considered photodoping (**Scheme 1a**) as a mechanism because the timescale of the long-lived donors is appropriate,[32] and n-doped QDs should be excellent electron donors. This mechanism was ultimately rejected because, as we will discuss below, there is no evidence for the presence of free carriers in the present work. We also considered that charge could be stored at ligated surface Cd (**Scheme 1b** and **c**), which best agrees with all our findings. Ligated surface metal ions can be reduced by external reductants,[33–35] so they may be susceptible to reduction by conduction band electrons.

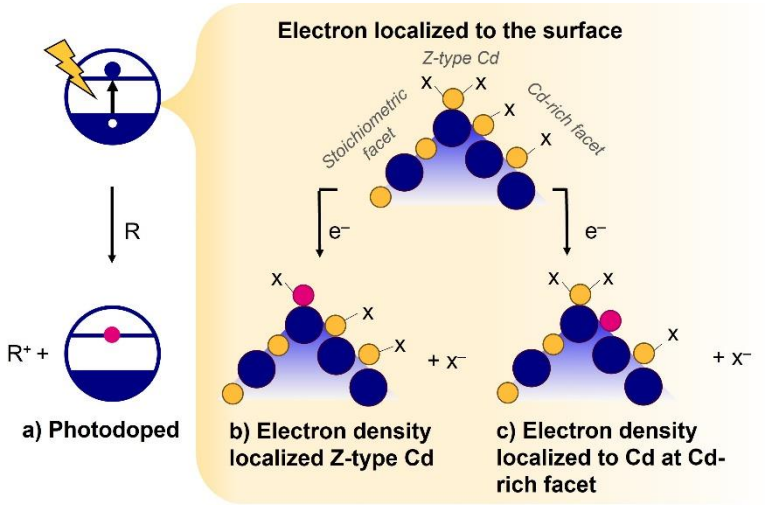

Scheme 1. Proposed mechanisms for electron storage. **(a)** n-type photodoping wherein a reducing agent (internal or external to the QD) quenches the photogenerated hole, leaving behind an electron in the conduction band. **(b)** Electron density localized to Z-type Cd, causing displacement of one ligand per electron stored. **(c)** Electron density localized to Cd on Cd-rich facets. (b,c) detail the localization of a photogenerated electron. Rapid localization of the corresponding hole [36–38] is not shown.

Results and Discussion

Electrons are stored locally rather than as conduction band charge carriers.

Previous work has demonstrated long-lived excited states or long-lived charge donors after illumination of QDs *via* photodoping. Chemical photodoping of QDs is a well-explored phenomenon wherein, after exciton generation, the hole is quenched by a reducing agent[39–42], leaving behind the electron as a free carrier in the conduction band, otherwise known as an n-type doped semiconductor (**Scheme 1a**). Generally, excess strong reducing agent, R, must be added to the system to generate electronically doped particles. However, we observed charge storage without any such chemical reductant being added. In one report, Shulenberger and coworkers demonstrated *native* photo-n-doping of CdS QDs.[43] During minutes of illumination, they observed an absorbance bleach at the excitonic transition, which was attributed to n-type photodoping, even without adding a reducing agent, which more closely mimics our observations. Especially relevant to our photo-electrochemical observation, the excess charges in photodoped QDs live for many minutes,[32] so we hypothesized that the long-lived charge donors we observed could be natively photodoped particles.

However, the observation of long-lived hole donors in our system, in addition to electron donors, conflicts with the photodoping hypothesis. To the best of our knowledge, stable p-type photodoped CdS QDs have not been experimentally prepared due to rapid hole localization at the QD surface. The same is true of related materials, including CdSe and PbS. If there was photodoping, we expect it to be n-type, so there should not be free holes. Initially, we postulated that in a natively photo-n-doped system, after excitation, the hole could be localized elsewhere (on the surface or the ligands as postulated by Shulenberger *et al.*), and this localized hole could act as a long-lived oxidizing agent we observe electrochemically.

To rule out the possibility of photodoping, we used optical spectroscopy after illumination to probe the presence of free conduction band electrons. Photodoping should cause bleaching of the first excitonic transition and quenching of band-edge photoluminescence.[44] Instead, during 30 minutes of illumination, we saw only very small (<1 nm) shifts in the lowest energy excitonic transition rather than a bleach (**Figure 2a**). These slight shifts resemble those others have observed upon surface charging and restructuring, causing an internal electric field known as the Stark effect.[45–48] We did not observe NIR absorption attributed to intraband excitation of conduction band electrons, which others have reported in photodoped QDs (**SI Figure 1**).

Of the CdS QDs investigated in this work, only those capped with (2-[2-(2-methoxyethoxy)ethoxy]ethyl)phosphonic acid (MEEEPA) had appreciable band-edge photoluminescence (See **SI Figure 2** for other surfaces). After 30 minutes of illuminating phosphonate-capped CdS QDs, the band-edge photoluminescence modestly increases in intensity, which is inconsistent with photodoping and is more consistent with photobrightening due to surface reconstruction[28] (**Figure 2b**). This reinforces that under our experimental conditions, the CdS QDs do not photodope, and therefore the long-lived stored charges are localized and not free carriers.

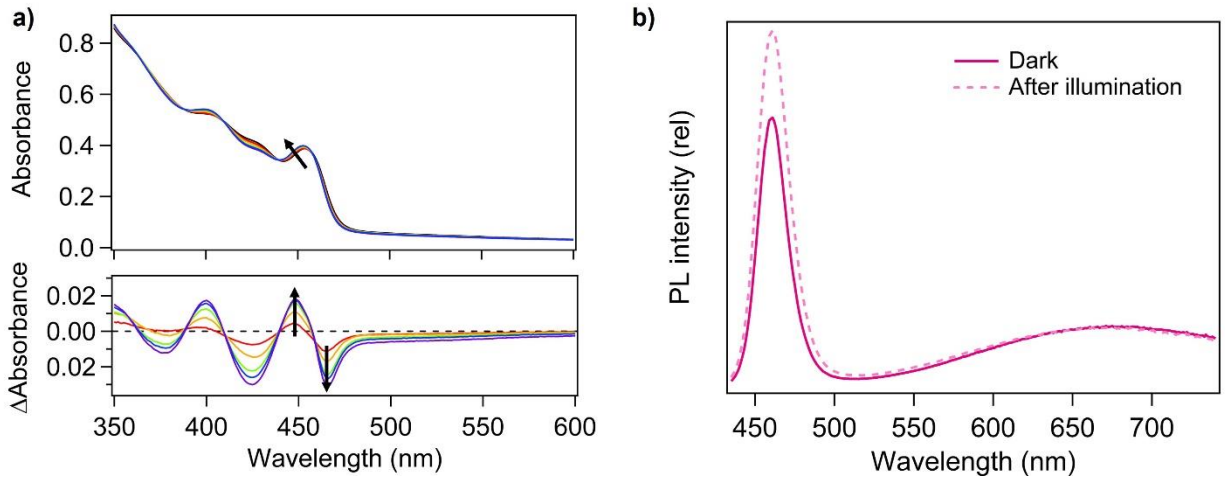

Figure 2. (a) UV-vis absorbance changes over 30 minutes of illumination of MEEEPA-capped CdS. **(b)** Photoluminescence brightening in MEEEPA-capped CdS after 30 minutes of illumination.

Three surface chemistries to assess the role of the QD surface in charge storage.

It is well documented that there are generally many types of surface sites on a Cd chalcogenide QD surface.[49–52] We have evidence from XPS that ours are no different as the Cd 3d lines are best fit to two Cd environments at the surface and the near-surface S/Cd atomic ratios are 1:1 within experimental error (see SI for details). Because of the distinct chemistries associated with Cd in different chemical environments, these surface sites should not necessarily be expected to have equivalent redox chemistry. For example, Hartley and Dempsey suggested that in PbS QDs, the Pb on the edges between facets were more likely to be reduced by cobaltocene than Pb on (111) or (100) facets.[34]

We were interested in probing which types of surface atoms are most likely to store electrons after illumination. To this end, we prepared QDs with three different surface chemistries and investigated their differences. We assessed the role of the head group of the ligands by comparing MEEEPA and 2-(2-methoxyethoxy)ethoxy acetic acid (MEEAA) capped CdS QDs. We assessed the role of surface stoichiometry by comparing MEEAA capped particles to MEEAA capped CdS QDs with lower Cd (and ligand) coverage prepared through surface etching. TEM and optical characterization of these different QDs can be found in **SI Figures 3** and **4**.

We characterized the surfaces of these three kinds of QDs by quantifying their ligand coverage with ^{1}H DOSY NMR (**Figure 3a**). We wanted to accurately quantify the ligand coverage, but needed to ensure that we were only counting ligands adsorbed to the QD surface and not including free ligands in solution. Quantitative DOSY NMR offers a technique where bound and free ligands are differentiated by their diffusion coefficient and can be used in cases where there is no simple spectroscopic handle to differentiate bound and freely diffusing species.[53] We used DOSY to quantify the ratio of bound and free ligands (**Figure 3b**) and then used an internal standard (mesitylene) to calculate the number of bound ligands per particle. We first found that the as-synthesized oleate capped QDs have 250 ligands per QD, which corresponds to 5 ligands/nm^2 (calculated using diameter from TEM and assuming spherical particles) and is consistent with literature reports and calculations of carboxylate ligand density.[52,54,55]

The short chain polyethylene glycol-terminated carboxylate and phosphonate ligands, MEEAA and MEEEPA, have 430 and 390 ligands per QD, which is approximately twice the number found in the oleate case. This gives ligand densities of 11 ligands/nm^2 and 7 ligands/nm^2, respectively. The higher density for MEEAA is consistent with previous observations of higher carboxylate than phosphonate density due to the diacidic nature of alkyl phosphonic acids.[56] These densities are far higher than any reported experimental or calculated ligand densities we have seen on CdS QDs. Furthermore, these are higher than the ligand density of a perfectly passivated cadmium-rich {100} surface of zinc blende CdS (5.76 ligand/nm^2, one ligand per surface Cd)[57]. This implies that the MEEAA and MEEEPA ligands cannot all have their head groups bound to the QD surface; some ligands are associated with the QD but not bound to the surface. We propose that the ligands form an interdigitated bilayer in these materials, where some head groups point out from the QD surface. Ligand bilayers have previously been constructed on nanocrystal surfaces with other ligands.[58–60]

We also made the QD surface less cation-rich by employing an established protocol wherein Z-type surface cadmium carboxylates were etched from the surface using diamines.[49] After etching, we exchanged the remaining ligands for MEEAA. After etching and then MEEAA ligand exchange, there were 39 MEEAA ligands per QD, or 0.9 ligands/nm^2. This extremely low ligand density, despite the large excess of MEEAA present in solution during ligand exchange, reinforces that we have effectively stripped the surface of Z-type Cd, decreasing the density of binding sites available to carboxylate.

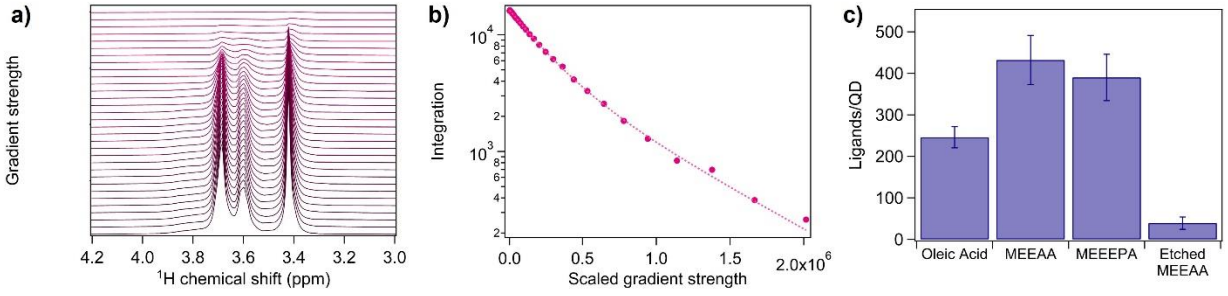

Figure 3. (a) ^{1}H DOSY NMR of MEEEPA capped CdS at 32 different gradient strengths. At higher gradient strengths, only signals from ligands bound to the QD surface are observed. **(b)**

Integration of the peaks in (a) plotted against the squared and scaled gradient strength. Data (circles) and fit to a biexponential decay (dotted line). **(c)** Results after using DOSY to determine the fraction of ligands in solution that are bound to CdS QDs with different ligands and surface stoichiometries. Error bars are from the propagation of uncertainty; see SI for details.

Chemical changes after illumination.

We considered that redox chemistry may promote charge storage on the surface ligands rather than the inorganic core, especially considering our non-conventional surface ligands bearing relatively weak C—O bonds. The report of native photodoping of CdS showed a ligand dependence on photodoping and invoked the double bond of oleic acid as a hole acceptor.[43] Similarly, a recent report found that when oleic acid capped CdSe QDs were irradiated with a 400 nm laser, the ligands desorbed from the QDs and fragmented to aldehydes, terminal alkenes, H_2, and water.[61] When we irradiated our MEEAA or MEEEPA capped CdS QDs for one hour, which is longer than the time to complete charge storage, we did not observe fragmentation of the ligand shell in the ^{1}H NMR spectrum. This confirms that charges are not stored by redox chemistry on the ligand backbone.

Analysis using DOSY did not show a significant difference in the fraction of ligands bound to the QD surface, though the estimated variance in this measurement was 60 ligands per QD. The only change in the ^{1}H NMR spectrum we noted was that the signal assigned to the protons alpha to the carboxylic acid in MEEAA had a small shift (0.01 ppm) further downfield after illumination (**SI Figure 5a**). Between different QD samples, we noticed that the chemical shift of this peak varied and was linearly correlated to the fraction of ligands in solution that were bound, as determined by DOSY (**SI Figure 5b**). This differs from archetypal NMR experiments using oleic acid capped QDs in nonpolar solvent, where bound and free ligands are observed as distinct resonances.[56,62–64] We assert that because the QD surface is in dynamic equilibrium, the observed chemical shift of this proton is a weighted average of protons on ligands bound to the QD surface and those on ligands freely diffusing in solution, as shown in **Equation 1**.

$$\delta_{obs} = \chi_{bound}\delta_{bound} + \chi_{free}\delta_{free} \quad \textbf{(Equation 1)}$$

Then, we can determine that a change in chemical shift from 3.8723 to 3.8881 ppm represents an 11% decrease in the bound fraction of ligands, or 48 fewer ligands bound per particle (see SI for calculations). Ligand dissociation after illumination is consistent with the reduction of ligated surface Cd (**Scheme 1b,c**), where surface reduction is locally charge compensated by X-type ligand dissociation.[33] The analogous protons alpha to the phosphonic acid in MEEEPA are not observed as a distinct resonance in the NMR spectra of the QDs, so an analogous interpretation was not possible.[65]

The hypothesis that stored charge is compensated by ligand dissociation is supported by a parallel set of electrochemical measurements where we irradiated MEEAA capped CdS solutions with and without electrolyte. As measured using cyclic voltammetry, the charge transfer rate after illumination ended was not significantly different between the two experiments, suggesting the presence of electrolyte did not impact charge storage (**SI Figure 6**). The lack of dependence on electrolyte further supports that charge storage is compensated intrinsically, i.e., by ligand loss.

This contrasts with work studying QD films, wherein electrolyte is necessary to stabilize surface charges,[66–69] presumably because ligand desorption is not a viable mechanism in the solid state.

When the MEEAA capped CdS QDs were irradiated overnight, they degrade. An insoluble grey powder formed and was identified as Cd^0 metal with large crystallite size by XRD (**Figure 4a**). Our coworkers recently also reported Cd^0 deposits formed during photocatalysis with CdS QDs.[70] Interestingly, UV-vis absorbance of the soluble fraction does not show that the QD size decreases even when insoluble Cd metal forms, suggesting degradation of the material does not evenly etch all particles (**SI Figure 7a**). DOSY NMR analysis of the soluble fraction showed that half as many of the ligands were bound. The signal assigned to the protons alpha to the carboxylic acid in MEEAA shifted further downfield (0.14 ppm) after overnight illumination (**Figure 4b**). We did see a few new minor peaks assigned to alcohol or ether degradation products (**SI Figure 7b**). In contrast, MEEEPA capped CdS QDs do not form Cd^0 deposits, and there are no changes to ligand binding observable by 1D or DOSY NMR.

Altogether, redox chemistry on the ligand backbone cannot be the primary site of charge storage, considering we don't observe these changes after one hour of illumination. In contrast, charge storage appears saturated by our electrochemical measurements after *ca.* 30 min. X-type ligand desorption is a mechanism for charge compensation of reduced surface sites in this system, at least in the case of the carboxylate capped QDs (**Scheme 1b,c**). Even under more extreme conditions like overnight irradiation of a QD solution, carboxylic acid capped QDs show Cd reduction and material degradation while phosphonate capped QDs do not measurably change. The ligand-dependent formation of Cd^0 and subsequent ligand desorption supports charge localization to ligated surface Cd atoms and suggests that these ligated surface Cd have different propensities for electron storage depending on the binding strength of the ligand.

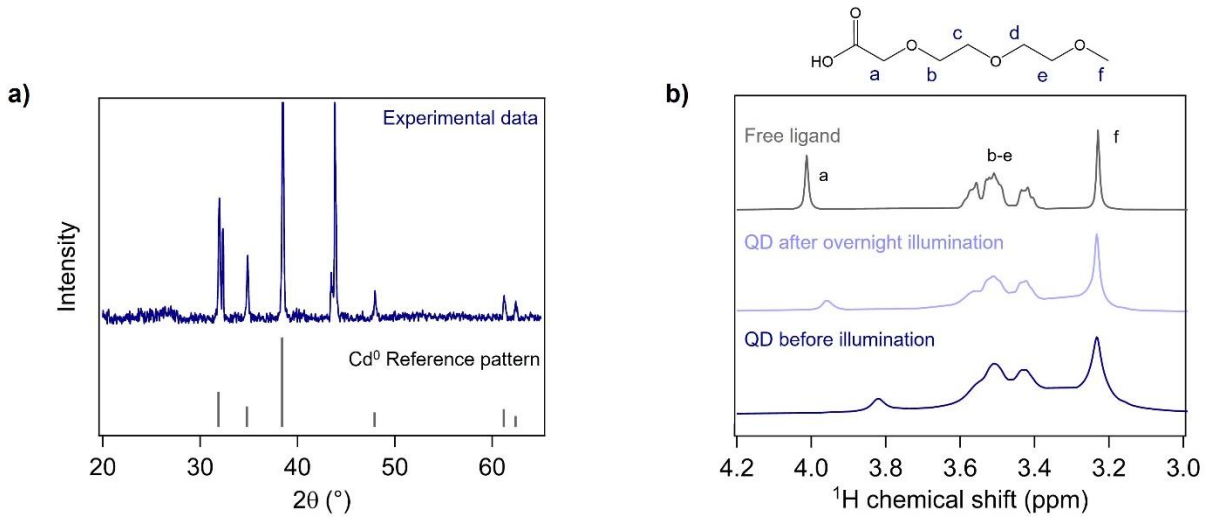

Figure 4. (a) XRD of the grey precipitate formed after illumination of MEEAA capped QDs overnight (top) compared to the reference pattern for hexagonal Cd^0. (**b)** The ^{1}H NMR spectrum of MEEAA (top) and MEEAA capped CdS QDs before (bottom) and after (middle) overnight illumination in DMSO-d_6, 300 MHz, d1=15s.

Long-lived charge donors observed electrochemically with all surfaces.

The observed rate of charge transfer from QDs was determined using photoelectrochemistry using cyclic voltammetry.[6] This measurement allows us to determine the observed rate of charge transfer (k_{obs}) from the magnitude of the CV distortion. Furthermore, we can track how this rate changes over time during extended illumination and after illumination ends. The changing k_{obs} over time gives insight into how charge donors form and are depleted over time as k_{obs} is related to the concentration of charge donors [QD*] and the intrinsic rate of charge transfer (k_{PCT}) by **Equation 2**. Assuming there is no change in the intrinsic rate over time, the variation of k_{obs} is linearly related to the number of charges stored. It is worth noting that k_{PCT} cannot be separately determined and varies between samples.

$$k_{obs} = [QD^*] \times k_{PCT} \quad \textbf{(Equation 2)}$$

In all samples, there is a rapid initial increase in k_{obs} after illumination starts but before the first scan is finished (50 s), which we hypothesize largely represents charge transfer that is not from stored charges, *i.e.,* from direct exciton dissociation (**Scheme 2a**). This is followed by a slow increase caused by the slow process of storing charges that are competent charge donors (**Scheme 2b**). When fitting this data to exponential curves, good fits were only obtained when the point at (0,0) was excluded, presumably because the fast initial rise in k_{obs} before the first scan is a distinct process from the slow charge storage. Analogously, k_{obs} quickly drops after illumination ends before the first scan is finished (50 s), then slowly decreases. As with the data during illumination, the decay results reinforce our hypothesis of two processes on different timescales: a rapid process completed before the first scan is taken and the slow decay of charge storage over many minutes, which is well-fit to an exponential curve.

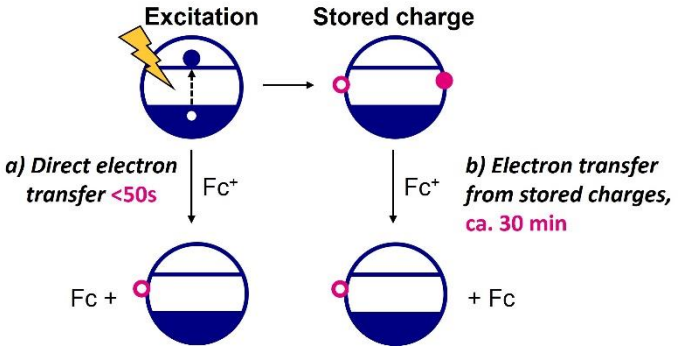

Scheme 2. Two pathways for charge transfer from QDs after excitation during the CV experiment. **(a)** Direct electron transfer that does not go through storage, *i.e.,* from exciton dissociation. Hole trapping in CdS QDs is very rapid, [36–38] so holes are likely trapped rather than left behind in the valence band after charge transfer. This mechanism reaches a maximum rate and ends within 50s of lights on/off. **(b)** Electron transfer from stored charges. This pathway lasts many minutes after illumination ends because of the long lifetime of stored charges.

We observe that MEEAA, MEEEPA, and etched MEEAA capped particles all have k_{obs} that slowly increase over *ca.* 30 min. Furthermore, charge transfer does not stop as soon as

illumination ends but instead takes at least 15 min to stop (**Figure 5**). Therefore, QDs with all three surface chemistries store charge. The raw CV data is available in **SI Figure 8**.

The magnitude of k_{obs} does vary between the QDs with different surfaces: MEEAA and MEEEPA capped QDs have the same k_{obs} within experimental variance, while the etched MEEAA sample has k_{obs} that is approximately twice as large as the others. The measured k_{obs} is inherently linked to the number of stored charges, as well as k_{PCT}, which depends on the permeability of the ligand shell and the driving force for charge transfer, among other factors. This means that comparing k_{obs} between samples does not directly inform on the relative number of charges that are stored, so while this measurement affirms charge storage in all samples, we needed a direct measurement of the number of stored charges to understand the dependence of charge storage on surface ligation.

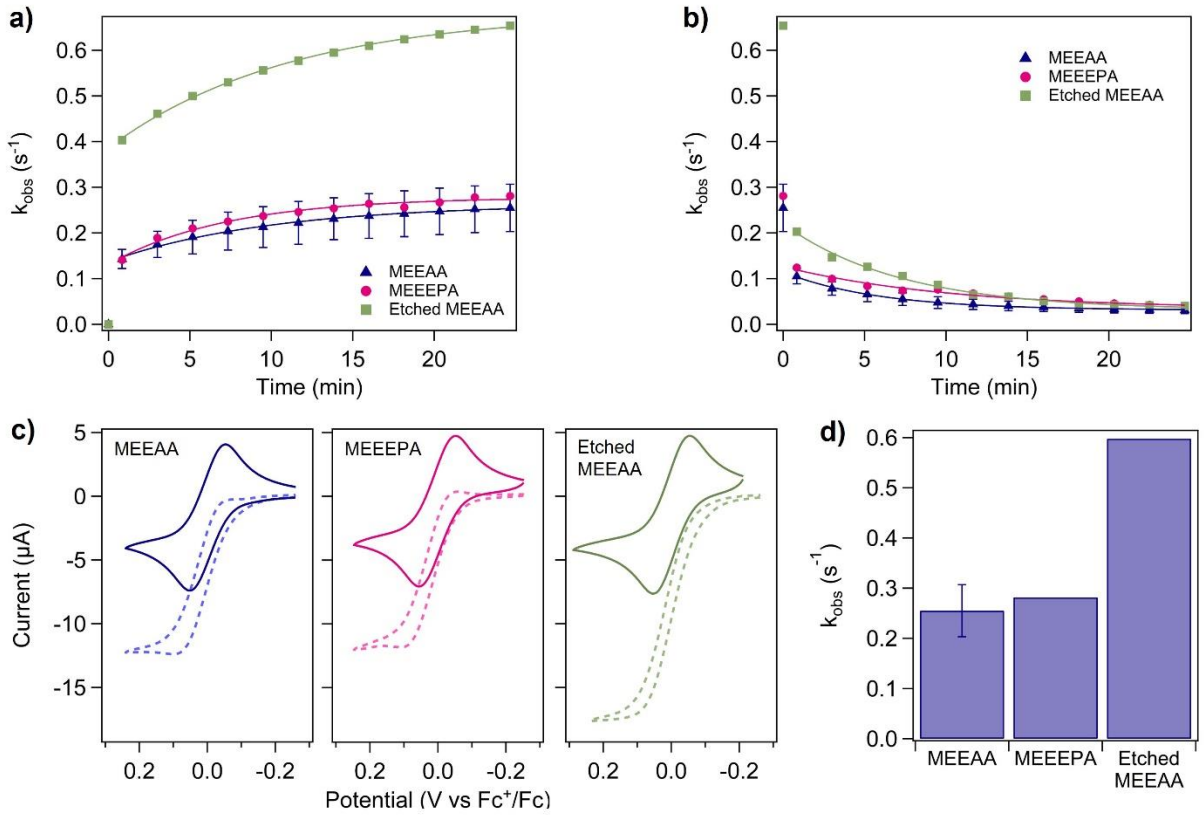

Figure 5. Comparison of the rate of electron transfer from CdS QDs with different surfaces. **(a,b)** The observed rate of electron transfer (k_{obs}) from CdS QDs to Fc^+ measured by cyclic voltammetry shows the slow increase in rate during minutes of illumination (a) and decay of electron transfer rate after illumination ends (b). The CdS QDs tested were MEEAA (blue triangles), MEEEPA (pink circles), and etched MEEAA (green squares). Lines between points are from fitting to an exponential function (details in SI). **(c)** Comparison of CVs before illumination (solid) compared to after 25 minutes of illumination (dashed) **(d)** The rate of electron transfer after 25 minutes of illumination for all three surface chemistries, obtained comparing the before and after CVs in (c). Error bars were obtained from triplicate measurements of the MEEAA sample.

Number of charges stored varies with QD surface.

Others interested in quantifying stored charges have used direct spectroscopic measurements of free carriers, including shifting plasmonic absorbance[10,71] or bleaching of excitonic features.[44,72] Because of the localized nature of the stored charges observed here, we are unable to use those methods. Others have observed long-lived stored charges in dark photocatalytic systems using XPS, wherein they can quantify the charges stored by observing reduced metal.[17] We were unable to observe redox changes to Cd or S in XPS after illumination of QD films, perhaps in part due to the low concentration of reduced species or similarity between the Cd^0 and Cd^{2+} binding energy (**SI Figure 9**).[73] Occasionally, EPR has been used to observe stored charge,[74,75] though we have not pursued this avenue. Still, others have quantified free carriers in doped nanocrystals using potentiometric titration, where an oxidizing agent is titrated, causing the solution's open circuit potential to shift.[40,41] This measurement requires many minutes for each point on the titration curve to stabilize open circuit potential, which sums to many hours to determine an equivalence point. Our electrochemistry data informs us that the stored charges live for less than *ca.* 30 minutes, so any measurement technique must take less time.

To quantify the number of charges stored, we aimed to titrate all stored charges with an excess of molecular acceptor (**Figure 6a**). This measurement does not rely on any spectroscopic changes to the QDs and is inherently only sensitive to charges stored that are competent charge donors. We first considered the use of dicationic methyl viologen, which, upon reduction by one electron, forms an intensely colored radical easily quantified with absorption spectroscopy. This substrate has been extensively studied as an electron acceptor from QDs[76–80] . It has even been used to quantify the formation of reduced metal species in colloidal suspensions of CdS and ZnS.[81–83] However, it is also well-documented that the reduced methyl viologen radical is a reasonably good Brønsted base, reacting with protons to yield non-colored products.[84–87] We did not observe the reduced radical in solutions containing MEEEPA capped QDs and we attribute this to degradation by the strongly acidic ligand. Because of this degradation pathway, it was not possible to use methyl viologen reduction to quantify the stored charges across the library of different QD surfaces.

Instead, we reacted the stored electrons with excess ferrocenium (Fc^+) to form ferrocene (Fc), which we selected due to its simple 1 e^- chemistry and the stability of the reduced form of the molecule. Furthermore, this is the same substrate used in our electrochemical experiments, which allows for clear comparison between k_{obs} and the number of stored charges. Because of the poor molar absorptivity of Fc, we monitored the formation of Fc using ^{1}H NMR spectroscopy, where the chemical shift of the peak corresponding to Fc and Fc^+ (observed as one peak due to rapid self-exchange, **Figure 6b**) can be related to the fraction of Fc^+ that was reduced (see Methods). We subtracted the number of Fc^+ reduced by QDs that had not been previously irradiated to control for different background reactivity. We note that the number of Fc formed is a lower bound of the number of electrons stored because some stored electrons may decay before they can react with Fc^+, and some Fc formed by stored electrons may be re-oxidized by stored holes (backward transfer).

All three surface chemistries studied did store charge, that is, previously irradiated QD samples formed more Fc than particles that had not been irradiated. We found that MEEAA capped particles stored the most charges (54 ± 7 per QD), while the etched particles stored fewer (31 ± 5 per QD) and the MEEEPA capped particles stored the fewest (9 ± 6 per QD) (**Figure 6c**). We note the similarity between the number of charges stored on the MEEAA capped QDs and the number of ligands we measured to desorb (48 per QD, discussed earlier). This suggests that for every stored electron, approximately one ligand is desorbed, which reinforces our proposed mechanism that electron donors are formed by the reduction of ligated surface Cd, charge-balanced by ligand desorption (**Scheme 1b,c**).

The quantification of stored charges does not mirror k_{obs} and reinforces the importance of measuring the number of stored charges in addition to their rate of transfer. The etched particles had twice the rate of charge transfer, but about half as many stored charges as regular MEEAA capped QDs. This is explained by the much higher permeability of the ligand shell (1/10 as many ligands), which is known to increase the rate of charge transfer due to the higher probability of collisions between QD inorganic surface and substrate.[88,89] Fewer charges stored on the etched particles confirms that some charge storage is at Z-type Cd (**Scheme 1b**), considering these are the species removed by the etching procedure. Notably, this does not rule out charge storage at Cd on Cd-rich surfaces (**Scheme 1c**); it may be that both kinds of ligated Cd may store charge.

We note that the MEEEPA capped QDs store far fewer charges than MEEAA, which further suggests the importance of surface ligands controlling the reactivity of surface Cd. MEEEPA binds more strongly to the QD surface, so presumably, it is a better Lewis base, making the Cd bound to it less Lewis acidic, decreasing the likelihood of electron localization. Surprisingly, despite the lower number of charges stored, MEEEPA and MEEAA capped QDs have the same k_{obs}. Because both ligand shells are very dense, ligand shell permeability cannot explain this discrepancy. We hypothesize that the lower number of stored charges (QD* in **Equation 2**) is balanced by the higher driving force for charge transfer (increasing k_{PCT} in **Equation 2**), leading to similar k_{obs}. Because of the indirect measurement of these stored charges, the relative energy of these states cannot be directly measured, though future work could use charge acceptors with different redox potentials to estimate this, analogously to Hartley and Dempsey.[34] Again, the dependence of the number of charges stored on the chemistry at ligated Cd supports the model presented in **Scheme 1b,c**. The much higher number of charges stored in MEEAA is consistent with our overnight illumination experiments where MEEAA but not MEEEPA capped CdS QDs form Cd^0 deposits and desorb ligands.

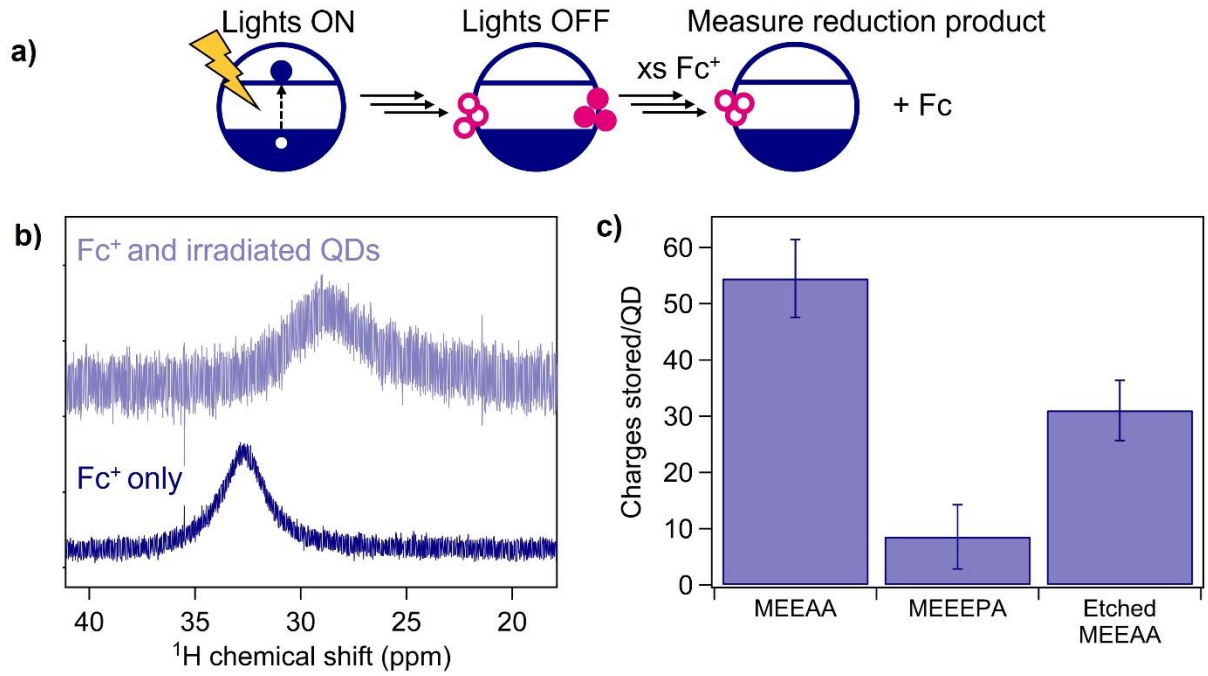

Figure 6. (a) Scheme for the measurement of stored charges. QDs were illuminated for 45 min, then the LED was turned off. 60 s after the illumination ended, a large excess of Fc^+ in CD_3CN was injected into the solution. **(b)** The observed ^1H NMR signal of Fc^+ (bottom) and a mixture of Fc^+ and Fc (top). The mixture is upfield and broadened compared to Fc^+ alone, and this shift is related to the mole fraction of Fc and Fc^+. 300 MHz, CD_3CN/PhCN 50:50 v:v. **(c)** The number of Fc^+ reduced to Fc per QD in solution for CdS QDs with different surfaces. Error bars from triplicate measurement.

Generality of charge storage.

We considered whether charge storage was unique to CdS QDs, so we synthesized InP and CdSe QDs that were also capped with MEEAA. InP is a III-V semiconductor that is more covalent than CdS or CdSe, which was especially interesting to us because the reactivity of ions in the lattice should be very different, though electron trapping at Z-type In is still a viable mechanism.[90] We performed identical cyclic voltammetry experiments under illumination and found that, as before, the CV distorted over slow timescales (See **SI Figure 10** for CV data). When CV data was interpreted to extract observed rates of charge transfer, we saw that charge transfer took many minutes to reach a maximum rate (Figure 7a), and charge transfer lasted for many minutes after illumination (**Figure 7b**). This was true for both electron transfer to ferrocenium (Fc^+) and hole transfer to cobaltocene (**SI Figure 11**). These results show the generality of the observation of charge storage.

The magnitudes of k_{obs} are difficult to directly compare between materials because of different band edge potentials, solution absorbance at the LED wavelength (solutions were normalized by concentration), QD size and diffusivity, ligand density, and other factors. However, the time constants from fitting the decay of k_{obs} are independent of those differences and can be

interpreted as the relative lifetimes of stored charges. InP has the longest-lived charges by far (τ = 25.5 ± 0.4 min), CdSe is intermediate (τ = 11.1 ± 0.5 min), and CdS has the shortest lifetime (τ = 7.2 ± 0.4 min). The difference between the different materials highlights the importance of the reactivity at the inorganic surface for charge storage. Furthermore, we posit that the high covalency in the InP lattice[91] might render redox changes to the QD surface less reversible, leading to the long lifetime of stored electrons.

We have determined that illumination causes storage of charge carriers for many minutes in all QD systems studied, spanning a variety of QD compositions, surface chemistries, and experimental conditions. Furthermore, while charge storage is sensitive to surface chemistry, charge storage is not directly based on localization to surface ligands, further generalizing this surprising phenomenon.

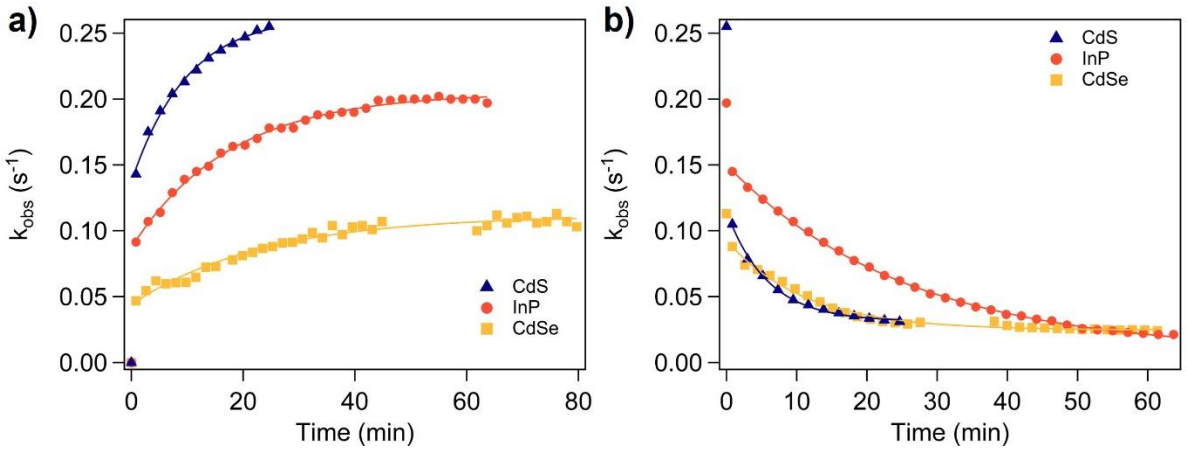

Figure 7. The observed rate of electron transfer (k_{obs}) from MEEAA capped QDs to Fc^+, measured by cyclic voltammetry under illumination. **(a)** The slow increase in electron transfer over time after illumination starts from CdS (blue triangles), InP (orange circles), and CdSe (yellow squares). **(b)** The decay of electron transfer over time after illumination ends from CdS (blue triangles), InP (orange circles), and CdSe (yellow squares). Lines between points are from fitting data to exponential functions, see SI for details.

Conclusions and Outlook

Photoinduced charge transfer from QDs is a critical process but cannot be explained by Marcus formalism and free carriers alone. We have shown that photoinduced charge transfer persists for many minutes after illumination ends, conflicting with the conventional viewpoint that charge transfer must compete with excitonic lifetimes. Furthermore, charges were stored in all QD systems we tested, including with or without electrolyte, using CdSe, InP, or CdS; using QDs capped with carboxylates or phosphonates, and using QDs with different surface stoichiometries. We devised a measurement for the number of charges stored *via* their reactivity with the electron acceptor, Fc^+. We emphasize the importance of measuring both the rate of stored charge transfer

using our electrochemical measurement and the number of stored charges when comparing different materials, as the observed rate depends on more than just the number of charge donors.

We found that charges are not stored as free carriers (e.g., as photodoped particles); similarly, charges are not stored *via* reactivity on the ligand backbone. We found that charge storage depended on the surface stoichiometry and the identity of the ligand head group, implying that charge is stored at the organic/inorganic interface on the QD surface. Furthermore, charge storage is intrinsically compensated by X-type ligand desorption. Because of this observation, as well as the dependence of the ligand on the number of charges stored, we propose that electrons are stored at ligated surface Cd. This paper did not investigate hole trapping, though we expect it to be trapped elsewhere on the surface. The electron and hole are trapped at separate sites, which is the origin of the extremely long-lived charge donors. There is likely a high kinetic barrier to the recombination of separately localized carriers.

We believe that others may have missed these intermediate states in QD charge transfer investigations because of the extremely long timescale of storage and depletion of stored charge and the subtle spectroscopic changes upon illumination. Despite the uniqueness of our observation, we do not view it as contradictory to other measurements of QD photophysics but rather as an extension of their behavior on longer timescales. QD luminescence blinking is a less understood photophysical phenomenon that also happens on longer timescales than other photophysical processes, and considering blinking is known to be turned off when the QD surface is electrochemically reduced,[31] we suspect that reversible charge storage at the QD surface may be tied to luminescence blinking. We encourage others to consider this surface-mediated mechanism moving forward.

Methods

General considerations. Unless otherwise noted, all manipulations were performed in an inert atmosphere glovebox. Additional experimental details may be found in the Supporting Information.

Photoelectrochemistry. 4 μmol of redox probe (Fc or cobaltocenium hexafluorophosphate) and either 30.8 nmol CdSe QD or 30.8 nmol InP QD or 9.5 nmol CdS QD were dispersed in 2.8 mL benzonitrile. The supporting electrolyte was 0.1M tetrabutyl ammonium hexafluorophosphate. The three electrode cell was assembled in a cuvette as we described earlier[6] and illuminated from the bottom using a 448 nm LED (from Luxeon Star, equipped with a 12° beam optic, FWHM 20 nm). The LED was driven at 0.5A, which corresponds to 0.77W.

Cyclic voltammograms were taken at 10 mV/s with a potential range of 500 mV. Sequential cyclic voltammograms were taken 30 seconds apart during charging and discharging. The observed rate of charge transfer (k_{obs} in s^{-1}) was calculated using equation 3.

$$\frac{i_c}{i_p} = \frac{1}{0.446}\sqrt{\frac{RT}{nF\nu}k_{obs}} \quad \text{(Equation 3)}$$

Where i_c is the plateau current (the current measured at highest potential for electron transfer or lowest potential for hole transfer for each scan), i_p is the peak current for the cyclic voltammogram taken without any light, n is the number of electrons transferred at the electrode, and ν is the scan rate in V/s.

DOSY. Diffusion ordered NMR spectroscopy was performed on a Bruker Avance-I spectrometer operating at 300.13 MHz proton frequency in DMSO-d_6. The instrument was equipped with a Bruker PABBI probe. The pulse program was stimulated echo and bipolar gradient pulses (stebpgp1s). The gradient strength was varied exponentially from 5-95% of the maximum gradient strength in 32 steps. A relaxation delay of 15s and a diffusion delay of $\Delta = 0.3$s were used. The gradient pulse duration was $\delta = 1500$ μs. The diffusion coefficients were extracted from the resulting DOSY data by fitting the decay the integration of the peak in question against the scaled gradient strength according to the Stejskal-Tanner equation (Q, defined in **Equation 3**) to a two-component exponential decay **(Equation 4).**

$$Q = (\gamma\,\delta\,g)^2\left(\Delta - \frac{\delta}{3}\right) \textbf{ (Equation 3)}$$

Where γ the gyromagnetic ratio of a proton and g is the gradient strength. The data to fit was obtained from integration in MestreNova v14 and then fit in Igor Pro v6.

$$I = A\exp(-D_1 Q) + B\exp(-D_2 Q) \textbf{ (Equation 4)}$$

Where I is the integration of the peak, D_1 and D_2 are the diffusion coefficients of the bound and free ligand in cm^2/s, and A and B reflect the relative molar content of the two components.

Quantification of stored charge by Fc^+ reduction. A 0.35 mL solution containing 10 nmol CdS QDs (concentration by optical spectroscopy) was illuminated in a mixture of benzonitrile/acetonitrile-d_3 for 45 minutes in a scintillation vial with magnetic stirring at 700 rpm. The illumination was stopped, then 60 seconds later 0.25 mL of solution containing 5 μmol $FcPF_6$ was added. This solution was transferred to an airfree NMR tube.

NMR was used to quantify the amount of Fc^+ that was reduced by the QDs. Because of the rapid electronic self-exchange between Fc (diamagnetic) and Fc^+ (paramagnetic), rather than observing two peaks, one for each species, we observe only one peak for both. This behavior is well-understood, and the mole fraction of Fc is related to position of the observed peak by **Equation 5.**

$$\chi_d = \frac{\delta_{dp} - \delta_p}{\delta_d - \delta_p} \textbf{ (Equation 5)}$$

Where δ_{dp} is the observed peak, δ_d is the NMR shift for Fc only (4.12 in CD_3CN/PhCN) and δ_p is the NMR shift of pure Fc^+ (32.70). Then the number of electrons transferred per quantum dot, Fc/QD, was calculated using the moles of $FcPF_6$ added as well as the moles of QD using **Equation 6.**

$$\frac{\text{Fc}}{\text{QD}} = \frac{\text{mol added FcPF}_6}{\text{mol QD}} \times \chi_d \textbf{ (Equation 6)}$$

Supporting Information

Electronic supplementary information (ESI) available: Additional experimental details, data processing and calculations, alternative mechanism discussion, and supplementary data. See DOI: XXXXXX.

Corresponding Author

*cossairt@uw.edu

Funding Sources

National Science Foundation MEM-C MRSEC DMR-1719797 and DMR-2308979.

Acknowledgements

This material is based upon work supported by the National Science Foundation under award numbers DMR-1719797 and DMR-2308979. Part of this work was conducted at the Molecular Analysis Facility, a National Nanotechnology Coordinated Infrastructure site at the University of Washington, which is supported in part by the National Science Foundation (grant NNCI-1542101), the University of Washington, the Molecular Engineering & Sciences Institute, and the Clean Energy Institute. NR Armstrong gratefully acknowledges the U.S. Department of Energy, Office of Science, Office of Basic Energy Sciences under award no. DE-SC0018285 and the Arizona Board of Regents for support of the surface characterization experiments.

References

(1) Kamat, P. V. Quantum Dot Solar Cells. The Next Big Thing in Photovoltaics. *J. Phys. Chem. Lett.* **2013**, *4* (6), 908–918. https://doi.org/10.1021/jz400052e.

(2) Livache, C.; Martinez, B.; Goubet, N.; Gréboval, C.; Qu, J.; Chu, A.; Royer, S.; Ithurria, S.; Silly, M. G.; Dubertret, B.; Lhuillier, E. A Colloidal Quantum Dot Infrared Photodetector and Its Use for Intraband Detection. *Nat. Commun.* **2019**, *10* (1), 2125. https://doi.org/10.1038/s41467-019-10170-8.

(3) Shirasaki, Y.; Supran, G. J.; Bawendi, M. G.; Bulović, V. Emergence of Colloidal Quantum-Dot Light-Emitting Technologies. *Nat. Photonics* **2013**, *7* (1), 13–23. https://doi.org/10.1038/nphoton.2012.328.

(4) Wilker, M. B.; Schnitzenbaumer, K. J.; Dukovic, G. Recent Progress in Photocatalysis Mediated by Colloidal II-VI Nanocrystals. *Isr. J. Chem.* **2012**, *52* (11–12), 1002–1015. https://doi.org/10.1002/ijch.201200073.

(5) Ye, C.; Zhang, D.-S.; Chen, B.; Tung, C.-H.; Wu, L.-Z. Interfacial Charge Transfer Regulates Photoredox Catalysis. *ACS Cent. Sci.* **2024**. https://doi.org/10.1021/acscentsci.3c01561.

(6) Homer, M. K.; Kuo, D.-Y.; Dou, F. Y.; Cossairt, B. M. Photoinduced Charge Transfer from Quantum Dots Measured by Cyclic Voltammetry. *J. Am. Chem. Soc.* **2022**, *144* (31), 14226–14234. https://doi.org/10.1021/jacs.2c04991.

(7) Cai, T.; Liu, Y.; Wang, L.; Dong, W.; Zeng, G. Recent Advances in Round-the-Clock Photocatalytic System: Mechanisms, Characterization Techniques and Applications. *J. Photochem. Photobiol. C Photochem. Rev.* **2019**, *39*, 58–75. https://doi.org/10.1016/j.jphotochemrev.2019.03.002.

(8) Savateev, O. Photocharging of Semiconductor Materials: Database, Quantitative Data Analysis, and Application in Organic Synthesis. *Adv. Energy Mater.* **2022**, *12* (21), 2200352. https://doi.org/10.1002/aenm.202200352.

(9) Hirakawa, T.; Kamat, P. V. Photoinduced Electron Storage and Surface Plasmon Modulation in Ag@TiO2 Clusters. *Langmuir* **2004**, *20* (14), 5645–5647. https://doi.org/10.1021/la048874c.

(10) Hirakawa, T.; Kamat, P. V. Charge Separation and Catalytic Activity of Ag@TiO2 Core−Shell Composite Clusters under UV−Irradiation. *J. Am. Chem. Soc.* **2005**, *127* (11), 3928–3934. https://doi.org/10.1021/ja042925a.

(11) Takai, A.; Kamat, P. V. Capture, Store, and Discharge. Shuttling Photogenerated Electrons across TiO2–Silver Interface. *ACS Nano* **2011**, *5* (9), 7369–7376. https://doi.org/10.1021/nn202294b.

(12) Liu, L.; Yang, W.; Li, Q.; Gao, S.; Shang, J. K. Synthesis of Cu2O Nanospheres Decorated with TiO2 Nanoislands, Their Enhanced Photoactivity and Stability under Visible Light Illumination, and Their Post-Illumination Catalytic Memory. *ACS Appl. Mater. Interfaces* **2014**, *6* (8), 5629–5639. https://doi.org/10.1021/am500131b.

(13) Ravikumar, M. P.; Bharathkumar, S.; Urupalli, B.; Murikinati, M. K.; Muthukonda Venkatakrishnan, S.; Mohan, S. Insights into the Photocatalytic Memory Effect of Magneto-Plasmonic Ag–Fe3O4@TiO2 Ternary Nanocomposites for Dye Degradation and H2 Production under Light and Dark Conditions. *Energy Fuels* **2022**, *36* (19), 11503–11514. https://doi.org/10.1021/acs.energyfuels.2c01563.

(14) EL-Sheshtawy, H. S.; El-Hosainy, H. M.; Shoueir, K. R.; El-Mehasseb, I. M.; El-Kemary, M. Facile Immobilization of Ag Nanoparticles on G-C3N4/V2O5 Surface for Enhancement of Post-Illumination, Catalytic, and Photocatalytic Activity Removal of Organic and Inorganic

Pollutants. *Appl. Surf. Sci.* **2019**, *467–468*, 268–276. https://doi.org/10.1016/j.apsusc.2018.10.109.

(15) Chiu, Y.-H.; Hsu, Y.-J. Au@Cu7S4 Yolk@shell Nanocrystal-Decorated TiO2 Nanowires as an All-Day-Active Photocatalyst for Environmental Purification. *Nano Energy* **2017**, *31*, 286–295. https://doi.org/10.1016/j.nanoen.2016.11.036.

(16) Liu, L.; Sun, W.; Yang, W.; Li, Q.; Shang, J. K. Post-Illumination Activity of SnO2 Nanoparticle-Decorated Cu2O Nanocubes by H2O2 Production in Dark from Photocatalytic "Memory." *Sci. Rep.* **2016**, *6* (1), 20878. https://doi.org/10.1038/srep20878.

(17) Li, Q.; Wai Li, Y.; Liu, Z.; Xie, R.; Ku Shang, J. Memory Antibacterial Effect from Photoelectron Transfer between Nanoparticles and Visible Light Photocatalyst. *J. Mater. Chem.* **2010**, *20* (6), 1068–1072. https://doi.org/10.1039/B917239D.

(18) Zhao, D.; Chen, C.; Yu, C.; Ma, W.; Zhao, J. Photoinduced Electron Storage in WO3/TiO2 Nanohybrid Material in the Presence of Oxygen and Postirradiated Reduction of Heavy Metal Ions. *J. Phys. Chem. C* **2009**, *113* (30), 13160–13165. https://doi.org/10.1021/jp9002774.

(19) Dong, F.; Xiong, T.; Sun, Y.; Zhao, Z.; Zhou, Y.; Feng, X.; Wu, Z. A Semimetal Bismuth Element as a Direct Plasmonic Photocatalyst. *Chem. Commun.* **2014**, *50* (72), 10386–10389. https://doi.org/10.1039/C4CC02724H.

(20) Chiou, Y.-D.; Hsu, Y.-J. Room-Temperature Synthesis of Single-Crystalline Se Nanorods with Remarkable Photocatalytic Properties. *Appl. Catal. B Environ.* **2011**, *105* (1), 211–219. https://doi.org/10.1016/j.apcatb.2011.04.019.

(21) J. Peterson, J.; D. Krauss, T. Photobrightening and Photodarkening in PbS Quantum Dots. *Phys. Chem. Chem. Phys.* **2006**, *8* (33), 3851–3856. https://doi.org/10.1039/B604743B.

(22) Chon, J. W. M.; Zijlstra, P.; Gu, M.; van Embden, J.; Mulvaney, P. Two-Photon-Induced Photoenhancement of Densely Packed CdSe⁄ZnSe⁄ZnS Nanocrystal Solids and Its Application to Multilayer Optical Data Storage. *Appl. Phys. Lett.* **2004**, *85* (23), 5514–5516. https://doi.org/10.1063/1.1829392.

(23) Bao, H.; Gong, Y.; Li, Z.; Gao, M. Enhancement Effect of Illumination on the Photoluminescence of Water-Soluble CdTe Nanocrystals: Toward Highly Fluorescent CdTe/CdS Core−Shell Structure. *Chem. Mater.* **2004**, *16* (20), 3853–3859. https://doi.org/10.1021/cm049172b.

(24) Jones, M.; Nedeljkovic, J.; Ellingson, R. J.; Nozik, A. J.; Rumbles, G. Photoenhancement of Luminescence in Colloidal CdSe Quantum Dot Solutions. *J. Phys. Chem. B* **2003**, *107* (41), 11346–11352. https://doi.org/10.1021/jp035598m.

(25) Asami, H.; Abe, Y.; Ohtsu, T.; Kamiya, I.; Hara, M. Surface State Analysis of Photobrightening in CdSe Nanocrystal Thin Films. *J. Phys. Chem. B* **2003**, *107* (46), 12566–12568. https://doi.org/10.1021/jp035484a.

(26) Hess, B. C.; Okhrimenko, I. G.; Davis, R. C.; Stevens, B. C.; Schulzke, Q. A.; Wright, K. C.; Bass, C. D.; Evans, C. D.; Summers, S. L. Surface Transformation and Photoinduced Recovery in CdSe Nanocrystals. *Phys. Rev. Lett.* **2001**, *86* (14), 3132–3135. https://doi.org/10.1103/PhysRevLett.86.3132.

(27) Cordero, S. R.; Carson, P. J.; Estabrook, R. A.; Strouse, G. F.; Buratto, S. K. Photo-Activated Luminescence of CdSe Quantum Dot Monolayers. *J. Phys. Chem. B* **2000**, *104* (51), 12137–12142. https://doi.org/10.1021/jp001771s.

(28) Carrillo-Carrión, C.; Cárdenas, S.; M. Simonet, B.; Valcárcel, M. Quantum Dots Luminescence Enhancement Due to Illumination with UV/Vis Light. *Chem. Commun.* **2009**, *0* (35), 5214–5226. https://doi.org/10.1039/B904381K.

(29) Krivenkov, V.; Samokhvalov, P.; Zvaigzne, M.; Martynov, I.; Chistyakov, A.; Nabiev, I. Ligand-Mediated Photobrightening and Photodarkening of CdSe/ZnS Quantum Dot Ensembles. *J. Phys. Chem. C* **2018**, *122* (27), 15761–15771. https://doi.org/10.1021/acs.jpcc.8b04544.

(30) Efros, Al. L.; Rosen, M. Random Telegraph Signal in the Photoluminescence Intensity of a Single Quantum Dot. *Phys. Rev. Lett.* **1997**, *78* (6), 1110–1113. https://doi.org/10.1103/PhysRevLett.78.1110.

(31) Galland, C.; Ghosh, Y.; Steinbrück, A.; Sykora, M.; Hollingsworth, J. A.; Klimov, V. I.; Htoon, H. Two Types of Luminescence Blinking Revealed by Spectroelectrochemistry of Single Quantum Dots. *Nature* **2011**, *479* (7372), 203–207. https://doi.org/10.1038/nature10569.

(32) Tsui, E. Y.; Carroll, G. M.; Miller, B.; Marchioro, A.; Gamelin, D. R. Extremely Slow Spontaneous Electron Trapping in Photodoped N-Type CdSe Nanocrystals. *Chem. Mater.* **2017**, *29* (8), 3754–3762. https://doi.org/10.1021/acs.chemmater.7b00839.

(33) Hartley, C. L.; Dempsey, J. L. Electron-Promoted X-Type Ligand Displacement at CdSe Quantum Dot Surfaces. *Nano Lett.* **2019**, *19* (2), 1151–1157. https://doi.org/10.1021/acs.nanolett.8b04544.

(34) Hartley, C. L.; Dempsey, J. L. Revealing the Molecular Identity of Defect Sites on PbS Quantum Dot Surfaces with Redox-Active Chemical Probes. *Chem. Mater.* **2021**. https://doi.org/10.1021/acs.chemmater.1c00520.

(35) Hartley, C. L.; Kessler, M. L.; Dones Lassalle, C. Y.; Camp, A. M.; Dempsey, J. L. Effects of Ligand Shell Composition on Surface Reduction in PbS Quantum Dots. *Chem. Mater.* **2021**, *33* (22), 8612–8622. https://doi.org/10.1021/acs.chemmater.1c01810.

(36) Wu, K.; Du, Y.; Tang, H.; Chen, Z.; Lian, T. Efficient Extraction of Trapped Holes from Colloidal CdS Nanorods. *J. Am. Chem. Soc.* **2015**, *137* (32), 10224–10230. https://doi.org/10.1021/jacs.5b04564.

(37) Ye, Y.; Wang, X.; Ye, S.; Xu, Y.; Feng, Z.; Li, C. Charge-Transfer Dynamics Promoted by Hole Trap States in CdSe Quantum Dots–Ni2+ Photocatalytic System. *J. Phys. Chem. C* **2017**, *121* (32), 17112–17120. https://doi.org/10.1021/acs.jpcc.7b05061.

(38) Rowland, C. E.; Schaller, R. D. Exciton Fate in Semiconductor Nanocrystals at Elevated Temperatures: Hole Trapping Outcompetes Exciton Deactivation. *J. Phys. Chem. C* **2013**, *117* (33), 17337–17343. https://doi.org/10.1021/jp405616u.

(39) Widness, J.; Enny, D.; McFarlane-Connelly, K.; Miedenbauer, M.; Krauss, T.; Weix, D. CdS Quantum Dots as Potent Photoreductants for Organic Chemistry Enabled by Auger Recombination. **2022**. https://doi.org/10.26434/chemrxiv-2022-3x02c.

(40) Araujo, J. J.; Brozek, C. K.; Kroupa, D. M.; Gamelin, D. R. Degenerately N-Doped Colloidal PbSe Quantum Dots: Band Assignments and Electrostatic Effects. *Nano Lett.* **2018**, *18* (6), 3893–3900. https://doi.org/10.1021/acs.nanolett.8b01235.

(41) Araujo, J. J.; Brozek, C. K.; Liu, H.; Merkulova, A.; Li, X.; Gamelin, D. R. Tunable Band-Edge Potentials and Charge Storage in Colloidal Tin-Doped Indium Oxide (ITO) Nanocrystals. *ACS Nano* **2021**, *15* (9), 14116–14124. https://doi.org/10.1021/acsnano.1c04660.

(42) Hughes, K. E.; Hartstein, K. H.; Gamelin, D. R. Photodoping and Transient Spectroscopies of Copper-Doped CdSe/CdS Nanocrystals. *ACS Nano* **2018**, *12* (1), 718–728. https://doi.org/10.1021/acsnano.7b07879.

(43) Shulenberger, K. E.; Keller, H. R.; Pellows, L. M.; Brown, N. L.; Dukovic, G. Photocharging of Colloidal CdS Nanocrystals. *J. Phys. Chem. C* **2021**, *125* (41), 22650–22659. https://doi.org/10.1021/acs.jpcc.1c06491.

(44) Rinehart, J. D.; Schimpf, A. M.; Weaver, A. L.; Cohn, A. W.; Gamelin, D. R. Photochemical Electronic Doping of Colloidal CdSe Nanocrystals. *J. Am. Chem. Soc.* **2013**, *135* (50), 18782–18785. https://doi.org/10.1021/ja410825c.

(45) Colvin, V. L.; Alivisatos, A. P. CdSe Nanocrystals with a Dipole Moment in the First Excited State. *J. Chem. Phys.* **1992**, *97* (1), 730–733. https://doi.org/10.1063/1.463573.

(46) Norris, D. J.; Sacra, A.; Murray, C. B.; Bawendi, M. G. Measurement of the Size Dependent Hole Spectrum in CdSe Quantum Dots. *Phys. Rev. Lett.* **1994**, *72* (16), 2612–2615. https://doi.org/10.1103/PhysRevLett.72.2612.

(47) He, S.; Li, Q.; Jin, T.; Lian, T. Contributions of Exciton Fine Structure and Hole Trapping on the Hole State Filling Effect in the Transient Absorption Spectra of CdSe Quantum Dots. *J. Chem. Phys.* **2022**, *156* (5), 054704. https://doi.org/10.1063/5.0081192.

(48) Kobosko, S. M.; DuBose, J. T.; Kamat, P. V. Perovskite Photocatalysis. Methyl Viologen Induces Unusually Long-Lived Charge Carrier Separation in CsPbBr3 Nanocrystals. *ACS Energy Lett.* **2020**, *5* (1), 221–223. https://doi.org/10.1021/acsenergylett.9b02573.

(49) Anderson, N. C.; Hendricks, M. P.; Choi, J. J.; Owen, J. S. Ligand Exchange and the Stoichiometry of Metal Chalcogenide Nanocrystals: Spectroscopic Observation of Facile Metal-Carboxylate Displacement and Binding. *J. Am. Chem. Soc.* **2013**, *135* (49), 18536–18548. https://doi.org/10.1021/ja4086758.

(50) Boles, M. A.; Ling, D.; Hyeon, T.; Talapin, D. V. The Surface Science of Nanocrystals. *Nat. Mater.* **2016**, *15* (2), 141–153. https://doi.org/10.1038/nmat4526.

(51) Prather, K. V.; Stoffel, J. T.; Tsui, E. Y. Redox Reactions at Colloidal Semiconductor Nanocrystal Surfaces. *Chem. Mater.* **2023**, acs.chemmater.3c00481. https://doi.org/10.1021/acs.chemmater.3c00481.

(52) Singh, S.; Leemans, J.; Zaccaria, F.; Infante, I.; Hens, Z. Ligand Adsorption Energy and the Postpurification Surface Chemistry of Colloidal Metal Chalcogenide Nanocrystals. *Chem. Mater.* **2021**, *33* (8), 2796–2803. https://doi.org/10.1021/acs.chemmater.0c04761.

(53) Hiller, W. Quantitative Studies of Block Copolymers and Their Containing Homopolymer Components by Diffusion Ordered Spectroscopy. *Macromol. Chem. Phys.* **2019**, *220* (17), 1900255. https://doi.org/10.1002/macp.201900255.

(54) Calvin, J. J.; Ben-Moshe, A.; Curling, E. B.; Brewer, A. S.; Sedlak, A. B.; Kaufman, T. M.; Alivisatos, A. P. Thermodynamics of the Adsorption of Cadmium Oleate to Cadmium Sulfide Quantum Dots and Implications of a Dynamic Ligand Shell. *J. Phys. Chem. C* **2022**, *126* (30), 12958–12971. https://doi.org/10.1021/acs.jpcc.2c04223.

(55) Harris, R. D.; Amin, V. A.; Lau, B.; Weiss, E. A. Role of Interligand Coupling in Determining the Interfacial Electronic Structure of Colloidal CdS Quantum Dots. *ACS Nano* **2016**, *10* (1), 1395–1403. https://doi.org/10.1021/acsnano.5b06837.

(56) Ritchhart, A.; Cossairt, B. M. Quantifying Ligand Exchange on InP Using an Atomically Precise Cluster Platform. *Inorg. Chem.* **2019**, *58* (4), 2840–2847. https://doi.org/10.1021/acs.inorgchem.8b03524.

(57) Heiba, Z. K.; Mohamed, M. B.; Imam, N. G. Biphasic Quantum Dots of Cubic and Hexagonal Mn Doped CdS; Necessity of Rietveld Analysis. *J. Alloys Compd.* **2015**, *618*, 280–286. https://doi.org/10.1016/j.jallcom.2014.08.106.

(58) Ahmed, S.; Wunder, S. L. Effect of High Surface Curvature on the Main Phase Transition of Supported Phospholipid Bilayers on SiO2 Nanoparticles. *Langmuir* **2009**, *25* (6), 3682–3691. https://doi.org/10.1021/la803630m.

(59) Fan, H.; Leve, E. W.; Scullin, C.; Gabaldon, J.; Tallant, D.; Bunge, S.; Boyle, T.; Wilson, M. C.; Brinker, C. J. Surfactant-Assisted Synthesis of Water-Soluble and Biocompatible Semiconductor Quantum Dot Micelles. *Nano Lett.* **2005**, *5* (4), 645–648. https://doi.org/10.1021/nl0500171.

(60) Rubio, J.; Izquierdo, M. A.; Burguete, M. I.; Galindo, F.; Luis, S. V. Photoluminescence of CdSe/ZnS Core–Shell Quantum Dots Stabilized in Water with a Pseudopeptidic Gemini Surfactant. *Nanoscale* **2011**, *3* (9), 3613–3615. https://doi.org/10.1039/C1NR10680E.

(61) Harvey, S. M.; Olshansky, J. H.; Li, A.; Panuganti, S.; Kanatzidis, M. G.; Hupp, J. T.; Wasielewski, M. R.; Schaller, R. D. Ligand Desorption and Fragmentation in Oleate-Capped

CdSe Nanocrystals under High-Intensity Photoexcitation. *J. Am. Chem. Soc.* **2024**, *146* (6), 3732–3741. https://doi.org/10.1021/jacs.3c10232.

(62) Fritzinger, B.; Capek, R. K.; Lambert, K.; Martins, J. C.; Hens, Z. Utilizing Self-Exchange To Address the Binding of Carboxylic Acid Ligands to CdSe Quantum Dots. *J. Am. Chem. Soc.* **2010**, *132* (29), 10195–10201. https://doi.org/10.1021/ja104351q.

(63) Kelm, J. E.; Dempsey, J. L. Metal-Dictated Reactivity of Z-Type Ligands to Passivate Surface Defects on CdSe Nanocrystals. *J. Am. Chem. Soc.* **2024**. https://doi.org/10.1021/jacs.3c11811.

(64) Kessler, M. L.; Kelm, J. E.; Starr, H. E.; Cook, E. N.; Miller, J. D.; Rivera, N. A.; Hsu-Kim, H.; Dempsey, J. L. Unraveling Changes to PbS Nanocrystal Surfaces Induced by Thiols. *Chem. Mater.* **2022**, *34* (4), 1710–1721. https://doi.org/10.1021/acs.chemmater.1c03888.

(65) Gomes, R.; Hassinen, A.; Szczygiel, A.; Zhao, Q.; Vantomme, A.; Martins, J. C.; Hens, Z. Binding of Phosphonic Acids to CdSe Quantum Dots: A Solution NMR Study. *J. Phys. Chem. Lett.* **2011**, *2* (3), 145–152. https://doi.org/10.1021/jz1016729.

(66) Boehme, S. C.; Wang, H.; Siebbeles, L. D. A.; Vanmaekelbergh, D.; Houtepen, A. J. Electrochemical Charging of CdSe Quantum Dot Films: Dependence on Void Size and Counterion Proximity. *ACS Nano* **2013**, *7* (3), 2500–2508. https://doi.org/10.1021/nn3058455.

(67) Chang, W. J.; Park, K.-Y.; Zhu, Y.; Wolverton, C.; Hersam, M. C.; Weiss, E. A. N-Doping of Quantum Dots by Lithium Ion Intercalation. *ACS Appl. Mater. Interfaces* **2020**, *12* (32), 36523–36529. https://doi.org/10.1021/acsami.0c09366.

(68) Sun, W.; Olikagu, C.; Carothers, K. J.; Pattadar, D.; Pyun, J.; Saavedra, S. S.; Armstrong, N. R. Waveguide-Based Spectroelectrochemical Characterization of Band Edge Energies in Submonolayers of CdSe Quantum Dots Tethered to Indium–Tin Oxide Electrodes. *J. Phys. Chem. C* **2022**. https://doi.org/10.1021/acs.jpcc.2c05692.

(69) Puntambekar, A.; Wang, Q.; Miller, L.; Smieszek, N.; Chakrapani, V. Electrochemical Charging of CdSe Quantum Dots: Effects of Adsorption versus Intercalation. *ACS Nano* **2016**, *10* (12), 10988–10999. https://doi.org/10.1021/acsnano.6b05779.

(70) Dou, F; Nishiwaki, E; Larson, H; Zion, T; Nguyen, H; Cossairt, B. Pathways of Quantum Dot Degradation during Photocatalysis. *ChemRxiv* **2024**. https://doi.org/10.26434/chemrxiv-2024-ds99w.

(71) Shubert-Zuleta, S. A.; Tandon, B.; Roman, B. J.; Gan, X. Y.; Milliron, D. J. How to Quantify Electrons in Plasmonic Colloidal Metal Oxide Nanocrystals. *Chem. Mater.* **2023**, *35* (10), 3880–3891. https://doi.org/10.1021/acs.chemmater.2c03694.

(72) Cohn, A. W.; Rinehart, J. D.; Schimpf, A. M.; Weaver, A. L.; Gamelin, D. R. Size Dependence of Negative Trion Auger Recombination in Photodoped CdSe Nanocrystals. *Nano Lett.* **2014**, *14* (1), 353–358. https://doi.org/10.1021/nl4041675.

(73) NIST X-Ray Photoelectron Spectroscopy Database. https://dx.doi.org/10.18434/T4T88K.

(74) Aschendorf, C. J.; Degbevi, M.; Prather, K. V.; Tsui, E. Y. EPR Spin Trapping of Nucleophilic and Radical Reactions at Colloidal Metal Chalcogenide Quantum Dot Surfaces. *Chem. Sci.* **2023**, *14* (45), 13080–13089. https://doi.org/10.1039/D3SC04724E.

(75) Keeble, D. J.; Thomsen, E. A.; Stavrinadis, A.; Samuel, I. D. W.; Smith, J. M.; Watt, A. A. R. Paramagnetic Point Defects and Charge Carriers in PbS and CdS Nanocrystal Polymer Composites. *J. Phys. Chem. C* **2009**, *113* (40), 17306–17312. https://doi.org/10.1021/jp9044429.

(76) Morris-Cohen, A. J.; Peterson, M. D.; Frederick, M. T.; Kamm, J. M.; Weiss, E. A. Evidence for a Through-Space Pathway for Electron Transfer from Quantum Dots to Carboxylate-Functionalized Viologens. *J. Phys. Chem. Lett.* **2012**, *3* (19), 2840–2844. https://doi.org/10.1021/jz301318m.

(77) Morris-Cohen, A. J.; Frederick, M. T.; Cass, L. C.; Weiss, E. A. Simultaneous Determination of the Adsorption Constant and the Photoinduced Electron Transfer Rate for a Cds Quantum Dot–Viologen Complex. *J. Am. Chem. Soc.* **2011**, *133* (26), 10146–10154. https://doi.org/10.1021/ja2010237.

(78) DuBose, J. T.; Kamat, P. V. Surface Chemistry Matters. How Ligands Influence Excited State Interactions between CsPbBr3 and Methyl Viologen. *J. Phys. Chem. C* **2020**, *124* (24), 12990–12998. https://doi.org/10.1021/acs.jpcc.0c03004.

(79) Zhao, F.; Li, Q.; Han, K.; Lian, T. Mechanism of Efficient Viologen Radical Generation by Ultrafast Electron Transfer from CdS Quantum Dots. *J. Phys. Chem. C* **2018**, *122* (30), 17136–17142. https://doi.org/10.1021/acs.jpcc.8b06551.

(80) Scholz, F.; Dworak, L.; Matylitsky, V. V.; Wachtveitl, J. Ultrafast Electron Transfer from Photoexcited CdSe Quantum Dots to Methylviologen. *ChemPhysChem* **2011**, *12* (12), 2255–2259. https://doi.org/10.1002/cphc.201100120.

(81) M. Gutierrez; A. Henglein. Photochemistry of Colloidal Metal Sulfides. 4. Cathodic Dissolution of CdS and Excess Cd2+ Reduction. *Berichte Bunsenges. Für Phys. Chem.* **1983**, *87*, 474–478.

(82) Reber, J. F.; Meier, K. Photochemical Production of Hydrogen with Zinc Sulfide Suspensions. *J. Phys. Chem.* **1984**, *88* (24), 5903–5913. https://doi.org/10.1021/j150668a032.

(83) Nedoluzhko, A. I.; Shumilin, I. A.; Nikandrov, V. V. Coupled Action of Cadmium Metal and Hydrogenase in Formate Photodecomposition Sensitized by CdS. *J. Phys. Chem.* **1996**, *100* (44), 17544–17550. https://doi.org/10.1021/jp9613807.

(84) Venturi, M.; Mulazzani, Q. G.; Hoffman, M. Z. Radiolytically-Induced One-Electron Reduction of Methyl Viologen in Aqueous Solution: Stability of the Radical Cation in Acidic and Highly Alkaline Media(1). *Radiat. Phys. Chem. 1977* **1984**, *23* (1), 229–236. https://doi.org/10.1016/0146-5724(84)90113-4.

(85) Bauer, R.; Werner, H. A. F. A New Mechanism for Electron Transfer between Methyl Viologen Radicals and Water. *J. Mol. Catal.* **1992**, *72* (1), 67–74. https://doi.org/10.1016/0304-5102(92)80031-B.

(86) Ebbesen, T. W.; Ferraudi, G. Photochemistry of Methyl Viologen in Aqueous and Methanolic Solutions. *J. Phys. Chem.* **1983**, *87* (19), 3717–3721. https://doi.org/10.1021/j100242a028.

(87) Mohammad, M.; Iqbal, R.; Khan, A. Y.; Bhatti, M.; Zahir, K.; Jahan, R. Protonation of Higher Reduction Products of Pyridinium Salts. *J. Phys. Chem.* **1981**, *85* (19), 2816–2820. https://doi.org/10.1021/j150619a023.

(88) Aruda, K. O.; Bohlmann Kunz, M.; Tagliazucchi, M.; Weiss, E. A. Temperature-Dependent Permeability of the Ligand Shell of PbS Quantum Dots Probed by Electron Transfer to Benzoquinone. *J. Phys. Chem. Lett.* **2015**, *6* (14), 2841–2846. https://doi.org/10.1021/acs.jpclett.5b01256.

(89) Knowles, K. E.; Tagliazucchi, M.; Malicki, M.; Swenson, N. K.; Weiss, E. A. Electron Transfer as a Probe of the Permeability of Organic Monolayers on the Surfaces of Colloidal PbS Quantum Dots. *J. Phys. Chem. C* **2013**, *117* (30), 15849–15857. https://doi.org/10.1021/jp406485y.

(90) Hughes, K. E.; Stein, J. L.; Friedfeld, M. R.; Cossairt, B. M.; Gamelin, D. R. Effects of Surface Chemistry on the Photophysics of Colloidal InP Nanocrystals. *ACS Nano* **2019**, *13* (12), 14198–14207. https://doi.org/10.1021/acsnano.9b07027.

(91) Heath, J. R. Covalency in Semiconductor Quantum Dots. *Chem. Soc. Rev.* **1998**, *27* (1), 65–71. https://doi.org/10.1039/A827065Z.

TOC Graphic